

Ground level enhancement events of Solar cycle 23

N Gopalswamy^{1,§}, H Xie², S Yashiro² & I Usoskin³

¹NASA Goddard Space Flight Center, Code 695, Greenbelt, MD 20771, USA

²The Catholic University of America, Washington DC 20064, USA

³Sodankylä Geophysical Observatory, Oulu University, FIN 90014, Finland

[§]E-mail: Nat.Gopalswamy@nasa.gov

Received 28 July 2010; accepted 18 August 2010

Ground level enhancement (GLE) events, typically in the GeV energy range, are the most energetic of solar energetic particle (SEP) events with the protons penetrating Earth's neutral atmosphere. During solar cycle 23, sixteen GLE events were observed with excellent data coverage of associated solar eruptions. The source of these GLE particles has been examined in this paper using white light observations of coronal mass ejections, type II radio bursts, and soft X-ray flares. It has been shown that the GLE events are consistent with shock acceleration in every single case. While the possibility of the presence of a flare component during GLE events cannot be ruled out, it can be definitely said that a shock component is present in all the GLE events. During 18 April 2001 GLE event, the source was located ~30 degrees behind the west limb, which is too far away from the magnetic field lines connecting Earth and hence the flare component can be ruled out. Also the presence of interplanetary shocks associated with the GLEs is shown using radio and *in-situ* observations.

Keywords: Ground level enhancement (GLE) event, Coronal mass ejection (CME), Solar flare, Shock, Solar energetic particle (SEP) event, Radio burst

PACS Nos: 96.60.ph; 96.60.qe; 96.60.Vg; 96.50.Fm

1 Introduction

Ground level enhancement (GLE) events are solar energetic particle (SEP) events that reach the neutral atmosphere of the Earth and produce secondary neutrons detected as sudden increases in cosmic ray intensity¹. The solar sources of the GLE events are energetic eruptions involving high speed coronal mass ejections (CMEs) and intense solar flares. CMEs drive fast-mode MHD shocks, which accelerate electrons and ions. Particles are also accelerated in the reconnection region of the eruption. From imaging observations of hard X-rays and gamma rays², one can infer that the angular extent over which the flare particles propagate is very small (~foot-point separation of gamma ray sources), while the CME-driven shock is much more extended. CME-driven shocks can also be inferred from metric and interplanetary (IP) type II radio bursts, which are also closely associated with SEP events^{3,4}. The GLE observations of solar cycle 23 have been used to combine the CME, flare and type II burst observations and present a global view of the events. A preliminary report was published with 14 GLEs in the 2005 ICRC proceedings⁵. This paper presents the complete set of

16 GLEs in solar cycle 23 with no more GLEs occurring as of mid 2008.

2 Observations

The list of GLE events available online at the Oulu Cosmic Ray Station (<http://cosmicrays oulu.fi/GLE.html>) has been used. The Oulu Neutron Monitor is part of the World Neutron Monitor Network and has been obtaining cosmic ray data since 1964 (ref. 6). It detects neutrons at rigidity above ~0.8 GV (the local vertical geomagnetic cut off rigidity). GLEs are identified as percentage of enhancement of the neutron monitor count above the background. During solar cycle 23, 16 GLE events were detected with intensities ranging ~3 - 269%. The first event occurred on 6 November 1997 and the last event occurred on 13 December 2006. There was a slight increase in the number of GLE events as one progressed from the rise (4 GLEs) to the maximum (5 GLEs) and to the declining phases (7 GLEs). Thus, no solar cycle variation can be inferred from the occurrence rate, which seems to depend on the existence of super active regions on the Sun, the prolific producers of CMEs⁷. For each GLE, one was

able to identify a unique CME observed by the Solar and Heliospheric Observatory (SOHO) mission's Large Angle and Spectrometric Coronagraph (LASCO) from http://cdaw.gsfc.nasa.gov/CME_list.

The source location of each CME was also identified based on the H-alpha flare location or from the EUV disturbances detected by the Extreme-ultraviolet Imaging Telescope (EIT) on board SOHO.

Figure 1 shows the CME and flare associated with the GLE on 13 December 2006. The CME originated from the southwest quadrant (S06W23) in active region NOAA 0930 (pointed by arrow) and was a fast CME (1774 km s^{-1}) that evolved into a halo CME. In Fig. 1(b), one can see the EUV disturbance around the solar source region. Projection correction using a cone model⁸ yielded a speed of $\sim 2164 \text{ km s}^{-1}$. The onset

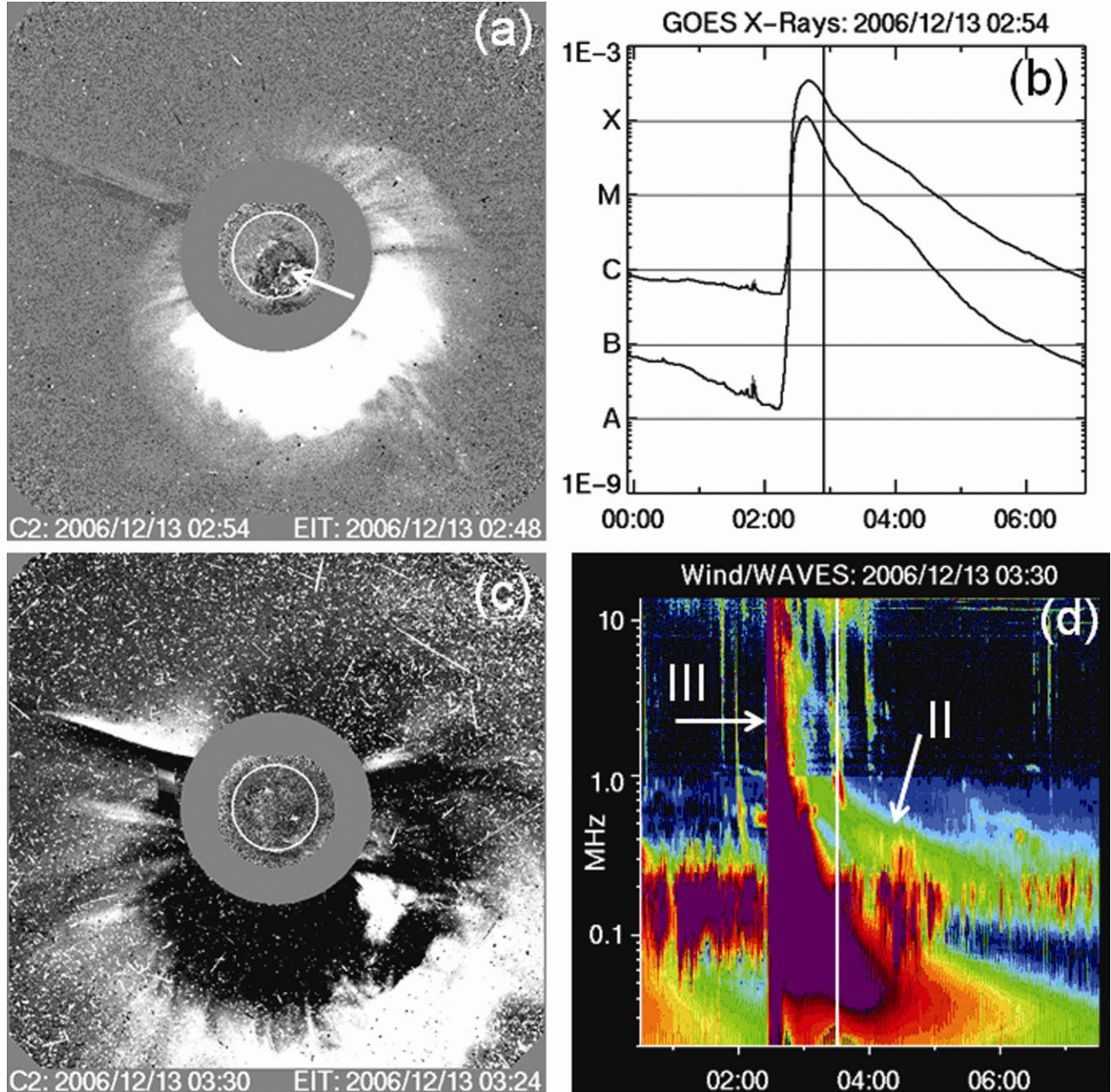


Fig 1 — CME (a, c), soft X-ray flare (b), and interplanetary type II burst (d) associated with the 13 December 2006 GLE event. The CME can be seen in the SOHO/LASCO difference images at 02:54 and 03:30 hrs UT with EIT difference images showing the disk activity. The approximate flare location is indicated by arrow. Vertical lines in the GOES plot and the Wind/WAVES dynamic spectrum mark the time of the corresponding LASCO frame on the left. Type II and type III bursts are marked by arrows in (d)

time of the CME is estimated to be ~02:21 hrs UT after deprojection. Note that the image at 03:30 hrs UT in Fig. 1(c) is already degraded due to SEPs arriving at the SOHO spacecraft moments after the CME's first appearance in the LASCO field of view [(02:54 hrs UT, Fig. 1(a)]. The X3.4 flare started around 02:17 hrs UT. The 4-minute delay of the CME may not be real because the CME was already at 5.3 solar radii when it first appeared, so the early acceleration phase was not observed. The Wind/WAVES radio dynamic spectrum [Fig. 1(d)] shows that the type II burst started a few minutes after the type III burst (02:24 hrs UT) at 14 MHz. However, the metric type II burst started as early as 02:26 hrs UT (Solar Geophysical Data). The IP type II burst continued down to ~150 kHz before fading but the shock was well observed in the Thermal Noise Receiver (TNR) dynamic spectrum at ~13:55 hrs UT on 14 December. The shock arrival at 1 AU was also marked by an energetic storm particle (ESP) event, which is an enhancement of locally accelerated particles detected as the shock spacecraft. The GLE itself was detected at 02:45 hrs UT by the Oulu neutron monitor and the intensity peaked at 03:05 hrs UT. The release time of the GLE particles at the Sun is calculated assuming a magnetic field line length of 1.2 AU. It takes ~11 min for ~1 GeV particles to travel this distance. To make it easier to compare, ~8 min have been subtracted for the light travel time to 1 AU (so as to be on par with the arrival

of electromagnetic signals at 1 AU) (ref. 9). This makes the GLE release time at the Sun as 02:42 hr UT. Clearly, both the flare and CME started well before the time of release of the GLE particles at the Sun. This procedure has been followed to gather information for all the GLE events of cycle 23.

There was no LASCO data for the GLE event of 24 August 1998 because SOHO was temporarily disabled around that time. However, there was an IP type II burst that lasted all the way to the local plasma frequency at Wind/WAVES, which means there should have been a powerful CME associated with this event. Solar wind plasma and magnetic field data clearly show CME material, confirming the existence of a CME in association with the GLE. For the GLE on 18 April 2001, the flare occurred behind the west limb, so there is no flare information. However, the active region is estimated to be ~30° behind the limb, based on its location on the disk before rotating behind the limb. The CME was well observed from above the southwest limb. Observations in X-rays, microwaves, and EUV all show that the source was behind the southwest limb¹⁰. The same active region produced another GLE event on 15 April when the active region was at S20W85.

Table 1 lists the 16 GLE events along with the properties of CMEs, flares, and radio bursts obtained. The dates and Earth onset times of the GLEs are listed in the table. The solar release time and peak time of GLEs listed are normalized to the Earth-arrival times

Table 1 — List of the 16 GLE events of solar cycle 23

Event #	GLE event date	GLE onset (Obs)	GLE onset (Inf)	Peak time, hrs UT	GLE Int, %	Type II onset, m	Type III onset, DH	Flare onset	Flare class/location	CME onset	CME ht, Rs	Sky speed, km s ⁻¹	Space speed, km s ⁻¹
1	06 Nov 1997	12:10	12:07	14:00	11.3	11:53	11:52	11:49	X9.4/S18W63	11:38	5.3	1556	1726
2	02 May 1998	13:55	13:52	14:05	6.8	13:41	13:35	13:31	X1.1S15W15	13:27	3.9	938	1332
3	06 May 1998	08:25	08:22	09:30	4.2	08:03	08:01	07:58	X2.7/S11W65	07:55	3.8	1099	1208
4	24 Aug 1998	22:50	22:47	02:05	3.3	22:02	22:04	21:50	X1.0/N35E09	DG	DG	DG	DG
5	14 Jul 2000	10:30	10:27	11:00	29.3	10:28	10:18	10:03	X5.7/N22W07	10:20	2.0	1674	1741
6	15 Apr 2001	14:00	13:57	14:35	56.7	13:47	13:49	13:19	X14/S20W85	13:34	3.4	1199	1203
7	18 Apr 2001	02:35	02:32	03:10	13.8	02:17	02:15	02:11	?/S23W117	02:08	6.6	2465	2712
8	04 Nov 2001	17:00	16:57	17:20	3.3	16:10	16:13	16:03	X1.0/N06W18	16:08	8.8	1810	1846
9	26 Dec 2001	05:30	05:27	06:10	7.2	05:12	05:13	04:32	M7.1/N08W54	05:05	4.4	1446	1779
10	24 Aug 2002	01:18	01:15	01:35	5.1	01:01	01:01	00:49	X3.1/S02W81	00:57	4.0	1913	1937
11	28 Oct 2003	11:22	11:19	11:51	12.4	11:02	11:03	11:00	X17/S20E02	11:04	4.5	2459	2754
12	29 Oct 2003	21:30	21:27	00:42	8.1	20:42	20:41	20:37	X10/S19W09	20:39	9.4	2029	2049
13	02 Nov 2003	17:30	17:27	17:55	7.0	17:14	17:16	17:03	X8.3/S18W59	17:19	3.0	2598	2981
14	17 Jan 2005	09:55	09:52	09:59	3.0	09:43	09:41	09:42	X3.8/N14W25	09:42	3.4	2547	2802
15	20 Jan 2005	06:51	06:48	07:00	277.3	06:44	06:45	06:39	X7.1/N14W61	06:41	3.2	3242	3675
16	13 Dec 2006	02:45	02:42	03:05	92.3	02:26	02:24	02:17	X3.4/S06W23	02:21	4.9	1774	2164

of electromagnetic signals. The percentage enhancement above background (GLE intensity), metric type II onset, decameter-hectometric (DH) type III onset, GOES soft X-ray flare onset, flare size (soft X-ray importance) with solar location, CME onset extrapolated from the CME height-time measurements, CME height (in solar radii, R_s) extrapolated to the GLE onset, Sky-plane speed of CMEs, and the deprojected CME speed using cone model are also listed. CME onset times were obtained by extrapolating the first appearance time in the LASCO field of view to the surface using the deprojected speed. The CME on 20 January 2005 was observed clearly only in one LASCO image, so the speed and onset was estimated by combining LASCO and EIT data⁵. The sky-plane speed was $\sim 3242 \text{ km s}^{-1}$, which becomes 3675 km s^{-1} , making the CME the fastest among the GLE associated CMEs. Four groups of events that originated from the same active region are: #2-3 from AR 8210, #6-7 from AR 9415, #11-13 from AR0486, and #14-15 from AR 0720.

3 Flare and CME properties

Table 1 shows that all the GLEs are associated with major soft X-ray flares. The smallest flare was M7.1 associated with the 21 December 2001 event (the only M-class event), while the largest one was the X17 flare on 28 October 2003. The size distribution of flares associated with GLE events has a median value of X3.8, compared to just C1.6 for that of all flares of cycle 23 (Fig. 2). Another compilation of 38 GLE events from 1964 to 1991 by Kudela *et al.*¹¹ showed that the optical importance ranged 1N-3B for the associated H-alpha flares. Thus, flares associated with GLEs are generally very large.

The solar sources in Table 1 are generally located from the disk center to the west limb. In fact, there were only 2 eastern events (E09 for 24 August 1998 event and E02 for the 28 October 2003 event) very close to the disk center. The fraction of eastern events is also very small (3 out of 38) in Kudela *et al.* compilation¹¹.

The average speed (Fig. 3) of GLE associated CMEs (1916 km s^{-1} in the sky plane) is greater than that of the SEP associated CMEs (sky-plane speed $\sim 1623 \text{ km s}^{-1}$). On the other hand, the GLE associated CMEs are more than 4 times faster than the average CME (460 km s^{-1} , which is the average of more than 11000 CMEs observed during the study period). The GLE associated CMEs constitute the fastest

population of CMEs. Note that the GLE events are a subset of the 80 SEP events shown in Fig. 3.

From Figs (2 and 3), it is clear that energetic flares and CMEs accompany all the GLE events, which means both processes (shock and flare reconnection) are expected to contribute to the observed GLE. It is, however, difficult to separate these components. It is, generally, no problem in understanding the production of particles in the flare process from hard X-ray, microwave, and gamma-ray observations. These are due to downward propagating particles, which typically occupy a small angular extent. For example, in the largest GLE event of solar cycle 23 on 20 January 2005, the hard X-ray foot-points were separated by $\sim 40 \text{ arcsec}$ (ref. 12). Even the H-alpha flare ribbons (tip to tip) have an extent of only 225 arcsec , which corresponds to $13^\circ.6$ (heliographic). This is close to the size of flux tubes that connect the

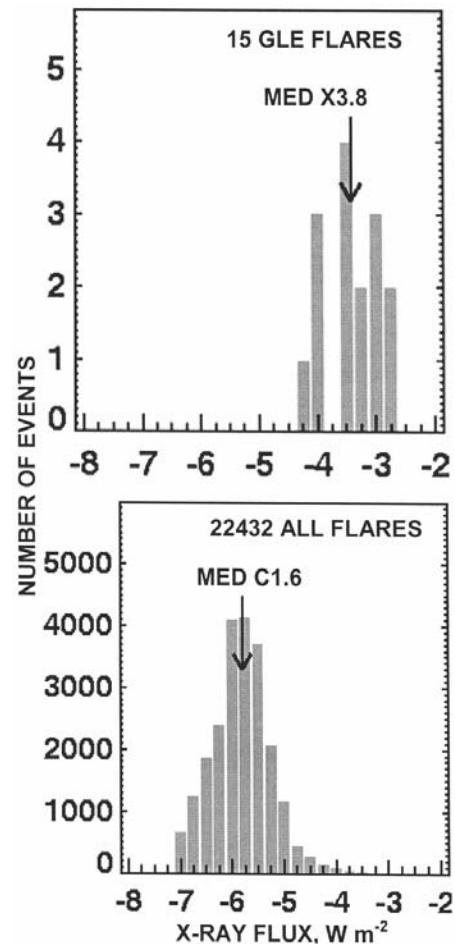


Fig. 2 — Distribution of soft X-ray flare sizes for 15 GLE events (top) and all flares during the study period (bottom). The median values of the distributions are indicated by arrows

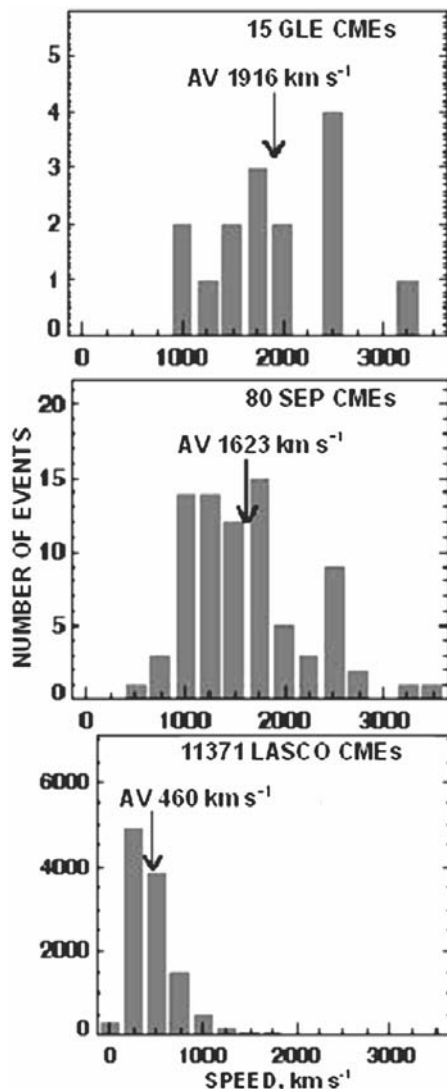


Fig. 3 — CME speed distributions for: GLE events (top); SEP events (middle); and all CMEs (bottom). The averages of the distributions are given on the plots

Sun and Earth. The widest dimension of the current sheet in which reconnection takes place and particles are accelerated cannot have an extent larger than this value. The gamma-ray foot-points are also separated by an extent similar to that of hard X-ray foot-points, although this could be slightly different². The outgoing particles may have a similar angular spread, which means flare particles maybe observed only for well-connected events. The principle is the same for impulsive SEP events, which originate from well-connected source regions. From this point of view, the 20 January 2005 GLE originated from N14W61, which is well connected. Some aspects of the GLE time profile such as a narrow peak with

highly anisotropic particles¹³ may indicate flare particles, while bulk of the particles are due to shock acceleration. Clearly, such cases are very rare because the 20 January 2005 event is the only one in cycle 23 that showed the anisotropic peak (H Moraal, private communication). Two other GLE events had similar source location (2 May 1998 event from W65 and 2 November 2003 event from W59). Both of these events were weak by two orders of magnitude compared to the 20 January 2005 event. Three such GLE events in cycle 22 and one from cycle 19 were reported many years ago¹⁴, all well-connected (W28 to W37).

If the spike component is excluded, all the GLE events are consistent with shock acceleration. Presence of fast and wide CMEs during each of the GLE event strongly indicates the existence of CME-driven shocks. The Alfvén speed in the corona, at heights where type II radio bursts form, is estimated to be in the range 400 – 1500 km s⁻¹ (ref. 15). Therefore, each one of the CMEs is likely to be super Alfvénic. The presence of a metric type II burst before the release of GLE particles also supports the existence of shocks in the corona. Finally, the presence of type II bursts at DH wavelengths indicates strong shocks, much stronger than cases where only metric type II bursts are present³. Table 2 shows the starting and ending times of DH type II bursts and their frequency extents (f1 – starting frequency and f2 – ending frequency in MHz). In most cases, the GLEs were released slightly before (3 to 33 min) the start of the DH type II burst and in a few cases slightly after (7 to 42 min). Note that in most cases the starting frequency is the highest observing frequency, which means one cannot tell at what frequency the burst really started. It can be anywhere up to the time of the metric type II burst. Most of the ending frequencies are below 0.1 MHz, which means the shocks were strong enough to produce electrons far into the interplanetary medium, often close to the observing spacecraft (at L1 point).

While one can understand that flare particles can propagate both towards and away from the Sun, it is not clear if the shock particles produce any observable signature at the solar surface. One of the reasons is the CME directly behind the shock, so the particles may not penetrate into the CME flux rope. The shock is also rapidly moving out (typically 1 Rs in 6 min). Therefore, it is more likely that the shock particles move predominantly away from the Sun.

4 CME height at GLE release

Now the CME location in the corona is considered when the GLE particles are released. The heliocentric distance of the CME is simply referred to as CME height. After projection correction, the CME height at first appearance is extrapolated to the time of the GLE release using the speed corrected for projection effects. The CME height at the time of GLE release ranges 2.0-9.4 Rs (Table 1). The distribution of CME heights at GLE release is compared with that at metric type II burst onset in Fig. 4. It is possible that the type II bursts originate from the flanks of the CME-driven shock, so the CME height represents the shock height only approximately. Nevertheless, the small CME height (1.8 Rs) at the time of metric type II burst means that CMEs have to travel an additional 2.9 Rs before releasing the GLE particles. Since the average speed of the GLE associated CMEs is $\sim 2000 \text{ km s}^{-1}$, the CMEs have to travel an additional 17 min before the release. The CMEs are also expected to have finished acceleration reaching the highest speed

when the GLE particles are released. Furthermore, the Alfven speed in the corona also starts falling below its peak value around 3 Rs (ref. 16). Therefore, the shock is likely to be the strongest around the time of the GLE release. If the anisotropic initial spike is from the flare site, the particles have to travel around the CME flux rope and pass through the CME-driven shock before arriving at Earth. Note also that the CME speed and the variation in Alfven speed with height are immaterial for the flare particles, which typically are released at $\sim 20,000 \text{ km}$ above the solar surface. It is not clear how the shock affects the flare particles. It is possible that they are further accelerated by the shock before reaching the observer.

5 Delay times

Figure 5 shows the delay of GLE release with respect to metric type II bursts, DH type III bursts, soft X-ray flares and CMEs. The median delay is the smallest with respect to the metric type II bursts (18 min) and the largest relative to the soft X-ray flares (27 min). The onset of DH type III bursts (delay = 19

Table 2 — Type II bursts in the Decameter-hecometric (DH) band from the Wind/WAVES Experiment

S No	DH-II Start		DH-II End		f1	f2
	Date	Time, hrs UT	Date	Time, hrs UT		
1	06 Nov 1997	12:20	07 Nov 1997	08:30	14	0.1
2	02 May 1998	14:25	02 May 1998	14:50	5 ^a	3.0
3	06 May 1998	08:25	06 May 1998	08:35	14	5.0
4	24 Aug 1998	22:05	26 Aug 1998	06:20	14	0.03
5	14 Jul 2000	10:30	15 Jul 2000	14:30	14	0.08
6	15 Apr 2001	14:05	16 Apr 2001	13:00	14	0.04
7	18 Apr 2001	02:55	18 Apr 2001	14:00	1 ^b	0.10
8	04 Nov 2001	16:30	06 Nov 2001	11:00	14	0.07
9	26 Dec 2001	05:20	27 Dec 2001	05:00	14	0.15
10	24 Aug 2002	01:45	24 Aug 2002	03:25	5	0.40
11	28 Oct 2003	11:10	29 Oct 2003	24:00	14	0.04
12	29 Oct 2003	20:55	29 Oct 2003	24:00	11	0.50
13	02 Nov 2003	17:30	03 Nov 2003	01:00	12	0.25
14	17 Jan 2005	09:25	17 Jan 2005	16:00	14	0.03
15	20 Jan 2005	07:15	20 Jan 2005	16:30	14	0.03
16	13 Dec 2006	02:45	13 Dec 2006	10:40	12	0.15

^aEarlier start possible f1 = 14 MHz at 14:06 hrs UT;
^bType II like event starts 14 MHz around 2:30 hrs UT

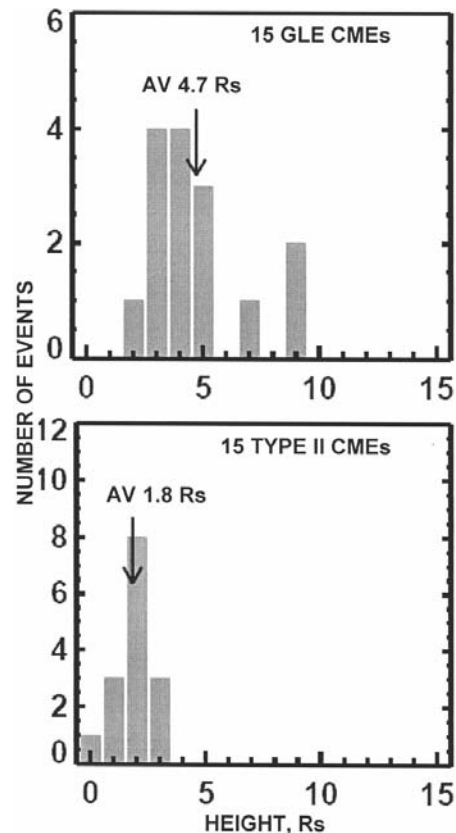


Fig. 4 — Distribution of CME height at the time of GLE release (top) and metric type II burst onset (bottom). The average values of the distribution are shown on the plots

min) is very close to that of type IIs. The delay relative to the CME onset (average 23 min) is intermediate. Thus, particle acceleration by both shocks (evidenced by the type II bursts) and flare reconnection (evidenced by type III bursts) seems to have started well before the GLE release. One may not be able distinguish between the mechanisms from the delay time alone.

6 GLE Event on 18 April 2001

The GLE on 18 April 2001 is unique during solar cycle 23 in that the source location was $\sim 30^\circ$ behind the west limb. SEPs are known to come from behind the west limb (Fig. 6). In a recent study, it was found that the SEP association of the behind the limb CMEs is similar to that of CMEs originating from $\sim W15$ considering the population of CMEs producing DH type II bursts¹⁷. A previous compilation of GLEs found that 9 GLE events (out of the 38) had their sources behind the west limb^{11,18}. During the current cycle, the rate is much lower, because only one out of the 16 GLEs originated from behind the west limb. The 18 April 2001 CME was exceptionally fast

(2465 km s^{-1} in sky plane and 2712 km s^{-1} deprojected). Given that high speed CMEs are generally associated with larger X-ray flares, one expects a large X-ray flare behind the limb. The event was, in fact, associated with an unusually large disturbance above the limb recorded in X-rays, EUV, and microwaves¹⁰.

Backsided events like the 18 April 2001 event provide strong evidence for shock acceleration because the flare source has an angular extent of only $\sim 13^\circ$, which means it is very difficult for the flare particles to arrive at Earth from behind the limb. On the other hand, CMEs are more extended (width $> 60^\circ$), so the shock front is expected to cross the sky plane to the front side. Similar argument applies to the poorly connected events erupting close to the disk center. It is highly likely that all the observed GLE particles are accelerated in the shock front in such events.

7 Summary and Conclusions

The GLE events of cycle 23 have been analysed, which is the first solar cycle that has extensive CME

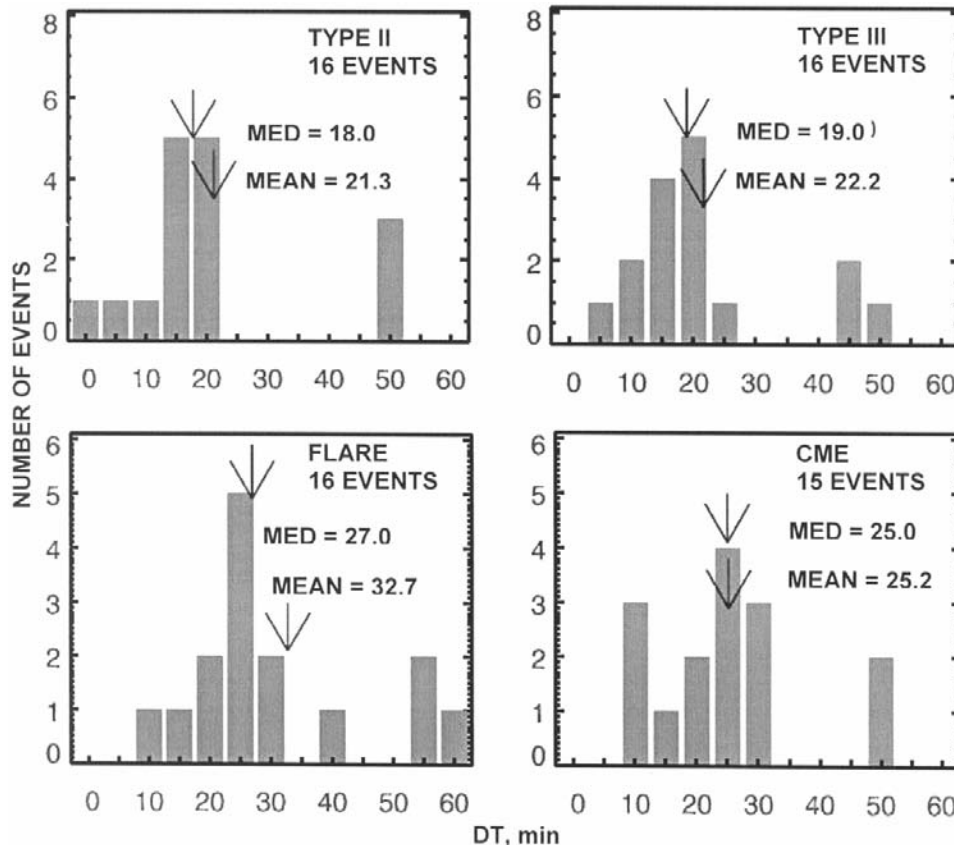


Fig. 5 — Delay of GLE release with respect to metric type II burst, DH type III burst, flare, and CME

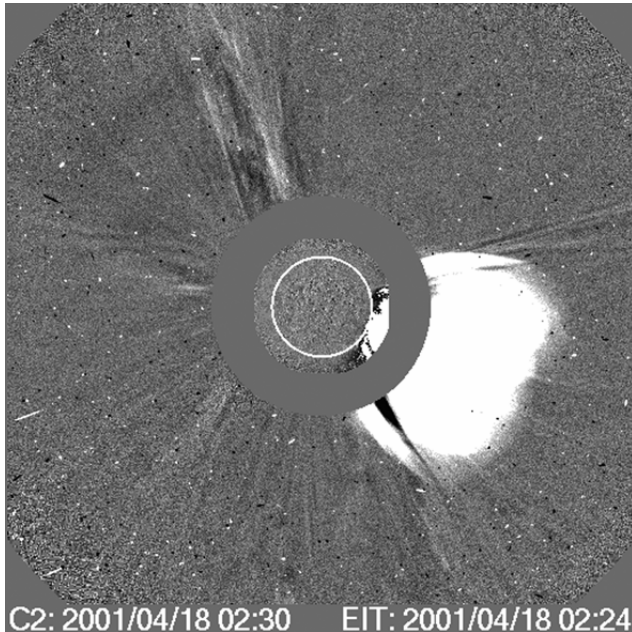


Fig. 6 — SOHO/LASCO C2 difference image with superposed EIT difference image showing the CME from behind the west limb. Note the EUV disturbance above the limb with nothing on the disk

observations for almost all the GLEs. There were only 16 GLE events in cycle 23, clearly demonstrating that these are rare events with an occurrence rate of only ~ 1.5 per year. The number of GLE events does not follow the solar cycle, but steadily increases from the minimum to the declining phases. The GLEs arise mostly from super active regions (such as AR 0486) that produce many CMEs in quick succession. The GLEs are a small subset of large SEP events, which total about 90 during cycle 23. Therefore, there is no surprise that the CME and flare properties of GLE events are similar to those of SEP events. In fact, the GLE associated CMEs are the fastest, the SEP associated CMEs being the second fastest. The flares are also very intense, being M7 or higher in X-ray importance (median X3.8). The CMEs are well under way by the time the GLEs are released (typically at a height of ~ 4.4 Rs) and have been driving shocks for at least 20 min. The solar eruptions associated with GLEs occur from near the disk center to locations well beyond the west limb. While it is difficult to tell the difference between flare and shock particles from the well-connected events, one can be sure of the shock particles for events from behind the limb. The same may be true of the poorly connected events from near the disk center. The extensive observations of flares and CMEs during the cycle 23 GLEs need to be further

exploited for a better understanding of these rare events.

Acknowledgments

Work supported by NASA's Living with a Star program is gratefully acknowledged.

References

- 1 Meyer P, Parker E N & Simpson J A, Solar cosmic rays of February 1956 and their propagation through interplanetary space, *Phys Rev (USA)*, 104 (1956) 768.
- 2 Lin R P, Particle acceleration by the Sun: Electrons, hard X-rays/Gamma-rays, *Space Sci Rev (Netherlands)*, 124 (2006) 233.
- 3 Gopalswamy N, Coronal mass ejections and type II radio bursts, in *Geophysical Monograph Series Volume 165: Solar eruptions and energetic particles* (American Geophysical Union, Washington DC), pp 207.
- 4 Cliver E W, Kahler S W & Reames D V, Coronal shocks and solar energetic proton events, *Astrophys J (USA)*, 605 (2004) 902.
- 5 Gopalswamy N, Xie H, Yashiro S & Usoskin I, *Coronal mass ejections and ground level enhancements: Proc. 29th International Cosmic Ray Conference*, Pune, edited by B Sripathi Acharya, S Gupta, P Jagadeesan, A Jain, S Karthikeyan, S Morris & S Tonwar (Tata Institute of Fundamental Research, Mumbai), 2005, 1, 169.
- 6 Usoskin I G, Mursula K, Kangas J & Gvozdevsky G, *On-line database of cosmic ray intensities: Proceedings of 27th International Cosmic Ray Conference* (Copernicus Gesellschaft, Germany), 2001, pp 1.
- 7 Gopalswamy N, Yashiro S & Akiyama S, *Coronal mass ejections and space weather due to extreme events: Proceedings of the ILWS Workshop Goa, India, 19-24 February 2006*, edited by N Gopalswamy and A Bhattacharyya (Quest Publications, Goa, India), 2006, 79.
- 8 Xie H, Ofman L & Lawrence G, Cone model for halo CMEs: Application to space weather forecasting, *J Geophys Res (USA)*, 109 (2004) A03109.
- 9 Kahler S W, Simnett G M & Reiner M J, *Onsets of solar cycle 23 ground level events as probes of polar energetic particle injections at the Sun: Proceedings of the 28th International Cosmic Ray Conference* (Tsukuba, Japan), 2003, pp 3415.
- 10 Gopalswamy N, *Radio observations of solar eruptions, Solar physics with the Nobeyama Radioheliograph: Proceedings of Nobeyama Symposium 2004* (Kiyosato, Japan, 26-29 October 2004), (Nobeyama Solar Radio Observatory, Japan), 2006, pp 81.
- 11 Kudela K, Shea M A, Smart D F & Gentile L C, *Relativistic solar particle events recorded by the Lomnický štít Neutron Monitor*, *Proc 23rd Cosmic Ray Conference* (Calgary, Canada), 3 (1993) 71
- 12 Grechnev V V *et al.*, An extreme solar event of 20 January 2005: Properties of the flare and the origin of energetic particles, *Sol Phys (Netherlands)*, 149 (2008) 149.
- 13 Butikofer R, Fluckiger E O, Desorgher L & Moser M R, *Proc 20th European Cosmic Ray Symposium* (Lisbon, Portugal), s0 (2006) 138.

- 14 Shea M A & Smart D F, *Unusual intensity-time profiles of ground-level solar proton events, AIP Conference Proceedings* (American Institute of Physics, Woodbury, NY, USA), 374 (1996), 131.
- 15 Gopalswamy N, Yashiro S, Xie H, Akiyama S, Aguilar-Rodriguez E, Kaiser M L, Howard R A & Bougeret J -L, Radio-quiet fast and wide coronal mass ejections, *Astrophys J (USA)*, 674 (2008) 560.
- 16 Gopalswamy N, Yashiro S, Akiyama S, Mäkelä P, Xie H, Kaiser M L Howard R A & Bougeret J-L, Coronal mass ejections, type II radio bursts, and solar energetic particle events in the SOHO era, *Ann Geophys (Germany)*, 26 (2008) 3033.
- 17 Gopalswamy N, Lara A, Kaiser M L & Bougeret J L, Near-Sun and near-Earth manifestations of solar eruptions, *J Geophys Res (USA)*, 106 (2001) 25261.
- 18 Cliver E W, The unusual relativistic solar proton events of 1979 August 21 and 1981 May 10, *Astrophys J (USA)*, 639 (2006) 1206.